Time-integrated optical emission studies of plumes generated from laser ablated germania glass

Paul J. Wolf[a]
Frank J. Seiler Research Laboratory, Materials Physics Division, 2354 Vandenberg Drive, Suite 6H79, USAF Academy, Colorado 80840-6272

(Received 3 February 1994; accepted for publication 9 April 1994)

The optical emission from plumes induced by ArF laser irradiation of GeO_2 was characterized as a function of laser fluence, distance from the target surface, and ambient O_2 pressure. Dispersion of the light emitted by the plume in a vacuum revealed emission from both neutral and singly ionized Ge atoms as well as neutral O atoms. The spatial variation showed that the ion concentration decreased exponentially from the target surface while the neutral atom number density reached peak intensities at distances of ≈1.5–2.5 cm from the target surface. Interactions between the plume constituents and the ambient molecular oxygen increased the excited Ge atom and Ge ion populations in the plume and, most notably, significantly enlarged the excited O atom concentration over that produced directly from the ablation process.

I. INTRODUCTION

Pulsed laser ablation has become a very successful method for depositing high-quality thin films and modifying surfaces. The congruent removal of material from a target and the relatively high kinetic energies of the plume constituents are important characteristics of this method that can influence thin-film growth processes.[1] Although much is known about the properties of films deposited under typical laser ablation conditions, knowledge is generally lacking in understanding the dynamics of laser generated plumes and the kinetics that govern thin film growth by this method. The collection, analysis, and interpretation of spectroscopic data obtained from plumes created above a surface irradiated by an intense laser pulse details the plume composition, the energy content of the ablation products, and the dynamics of the plume species which can subsequently lead to an improved understanding of the laser ablation phenomenon. In principle, the evolution of the plume can be theoretically predicted with an understanding of the initiation mechanisms and kinetic processes (electron temperature, electron density, ionization state, etc.).

The spatial and temporal evolution of transient species produced during the laser-target interaction, such as excited atoms, ions, and molecules, can be monitored as a function of the irradiation conditions, ambient gas pressure and composition, and the axial/radial distance from the target surface by investigating the optical emission produced in the plumes. Many of these spectroscopic studies have been performed near the target surface where interesting plasma dynamics can be explored. Recently, Mehlman *et al.*[2,3] reported results of a study in the vacuum ultraviolet to ultraviolet regions at distances less than 1 cm from the target surface aimed at obtaining insight into the early stages of the laser-target and laser-plasma interaction. In contrast, probing the plume at distances comparable to typical target-substrate separations (≈4–8 cm) should provide information on the dynamics of the laser ablated material immediately prior to collisions with a substrate surface. These studies are particularly important when reactive gases are required for stoichiometric film growth since the presence of this ambient gas can affect both the nature and the energy of the material impinging on the film growth surface. Reactive gases are commonly used to maintain the oxygen content in films produced in ablation experiments that employ oxidized targets such as YBaCuO.[4] The formation of metal-oxide diatomic molecules has been directly correlated with improved film stoichiometry and, in general, better film quality,[5] and the distant separation between the target and the substrate allows for potentially more gas-phase reactive encounters which can produce these species. Several optical emission studies have been performed to understand the ablation of high T_c superconducting materials that ultimately result in the transfer of material onto a substrate.[4–8] Although the bulk of both the temporal and time-integrated optical emission studies have been devoted to high T_c superconducting materials, optical emission spectroscopy has also been performed on other laser ablated materials such as carbon,[9] dielectrics,[10,11] metals such as Al,[2,3,12] and various polymers.[13]

Recently, stoichiometric GeO_2 films have been fabricated on ambient temperature substrates by ablating GeO_2 targets in 150 mTorr of O_2.[14] The high O_2 pressures required to form stoichiometric films suggested that gas phase reactions, in addition to the presence of energetic atomic species, may be important for incorporating stoichiometric quantities of oxygen in the film. Thus the purpose of this work was to study the dynamics of material ablated from a GeO_2 target in the presence of molecular oxygen to correlate the ablation process and the plume composition with the formation of stoichiometric thin films. The light emitted by a plume after ArF laser irradiation of a GeO_2 target was collected and analyzed using optical emission spectroscopy (OES). The time-integrated emission spectra were analyzed to identify the

[a]Present address: Dept. of Engineering Physics, Air Force Institute of Technology, Wright Patterson AFB, OH 45433.

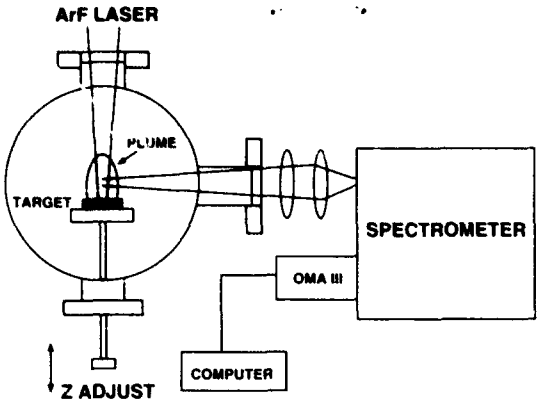

FIG. 1. Schematic diagram of the experimental arrangement.

composition of the plume, and the behavior of neutral and ionic species was mapped when variations were made in the O_2 pressure, laser fluence, and distance from the target surface. In a related study, Vega *et al.*[15] investigated the ablation products of a Ge target as a function of O_2 pressure. These experiments, however, were performed at distances less than 5 mm from the target surface and, therefore, could be insensitive to possible reactions occurring downstream.

II. EXPERIMENT

Figure 1 shows the experimental arrangement with the ablation chamber and the data collection system. The experiments were performed in a vacuum chamber that typically achieved a base pressure of 2×10^{-6} Torr with a turbomolecular pump. An ArF laser [$\lambda=193$ nm; 28 ns full width at half maximum (FWHM)] was focused at normal incidence onto the surface of a GeO_2 target to generate the plume. The laser fluence was varied between 0.5–6.5 J cm^{-2} during the experiments by adjusting the combination of the laser energy and the spot size on the target surface. All data were collected with laser repetition rates ≤ 1 Hz. The experiments were performed both in vacuum (2×10^{-6} Torr) and O_2 pressures ranging from 10^{-4} Torr to 200 mTorr which spanned the pressure range used in previous GeO_x thin-film growth studies.[14]

The target was mounted on an adjustable shaft which allowed translation perpendicular to the target surface. The optical emission was sampled at several locations from the front surface of the target, z, by moving the target away from the "0" position while simultaneously adjusting the laser focusing lens to keep the laser fluence constant. Distances from 0.2 to 5 cm were covered in these studies. The "0" position was determined empirically by translating the target until the collected intensity lost features associated with discrete or continuum emission.

The interaction of laser radiation with the target produced a visible plume extending normal to the target surface. The optical emission was collected normal to the plume's main expansion direction with a spherical lens positioned a focal length (23 cm) from the plume axis. A 15 cm focal length cylindrical lens subsequently focused the light onto a 100-μm-wide entrance slit of a 0.5 m spectrometer. The spectrometer was equipped with an linear diode array (PAR OMA III) to detect the spectrally resolved emission. A glass microscope slide was positioned in front of the spectrometer to eliminate second order uv lines from being recorded at wavelengths above 350 nm. The OMA III signal was recorded, stored, and analyzed on a computer. Several visible and UV emission lines were recorded in the following wavelength regions: 260 nm$\leq\lambda\leq$340 nm in 20 nm increments; 420 nm$\leq\lambda\leq$520 nm in 20 nm increments; and 580, 600, and 780 nm. These spectral regions were chosen based on the known spectral line positions of neutral Ge atoms (Ge I),[16] singly ionized Ge atoms (Ge II),[16] molecular GeO,[17] and neutral O atoms (O I).[18] Ten laser shots were required to achieve good signal-to-noise ratios in these experiments. The light collection system was not calibrated for absolute intensity measurements since only relative intensities were important in this work. The intensity of each spectral line was obtained by simply measuring peak heights after correcting for baseline variations.

The ablation rate of GeO_2 was also measured as a function of the incident laser energy density by irradiating fixed targets in vacuum. The laser fluence on target was determined by measuring the total energy delivered by the laser to the target position through all the optics and dividing this value by the area of the laser spot on the target. The crater depths were measured with a surface profiler at several locations along the length of the crater to obtain averaged values. The material removal rate was subsequently plotted as depth/pulse versus laser fluence.

III. RESULTS

A. GeO_2 ablation rate

Germanium dioxide targets were irradiated at energy densities between 0.5 and 7.0 J cm^{-2}. Well defined craters with 10–15 μm hole depths were produced on the target surface using 50–80 laser pulses at fluences F above 2 J cm^{-2}. At fluences between 1–2 J cm^{-2}, 75–100 laser pulses were required to achieve measurable crater depths. The irradiated areas at $F<1$ J cm^{-2} formed very shallow craters and they appeared to be heat damaged on the surface as opposed to other irradiated sites produced with higher laser fluences which clearly showed crater formation. The difficulty in measuring the area of these indentations over large laser spot sizes introduced large relative errors in the mass removal rates at $F\leq1$ J cm^{-2}. Figure 2 shows the results plotted as crater depth in μm per laser pulse versus laser fluence. The data in Fig. 2 were fit to a phenomological expression for the ablated depth as a function of fluence described in Eq. (1):

$$d=\alpha^{-1}\ln(F/F_{\text{threshold}}), \tag{1}$$

where d is the crater depth, α is the absorption coefficient at 193 nm, and $F_{\text{threshold}}$ is the ablation threshold fluence. As shown in Fig. 2, this expression produced a reasonable fit to the data with an absorption coefficient of 1.3×10^5 cm^{-1} and

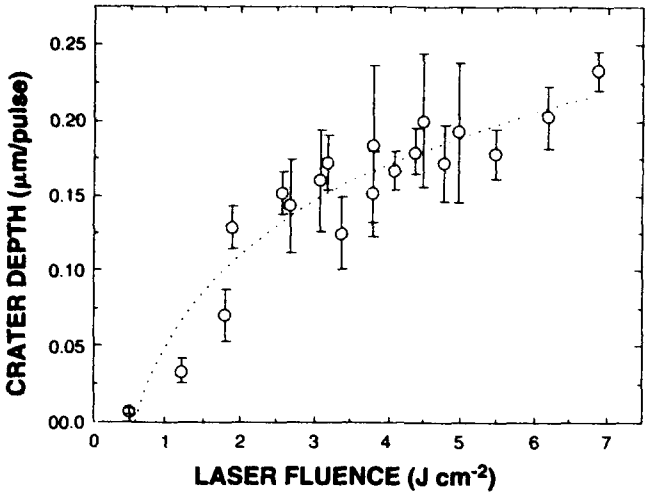

FIG. 2. The crater depth per laser pulse as a function of laser fluence for GeO_2 targets irradiated in vacuum. The fit to the data produced a ablation threshold fluence of 0.46 J cm $^{-2}$.

a threshold fluence of 0.46 J cm^{-2}. The absorption coefficient from the fit was within 35% of the accepted value for GeO_2 at 193 nm.[19]

The ablation threshold determined using the above procedure was corroborated by examining the optical emission produced from laser ablated targets. By varying the laser fluence on the target and monitoring the intensities of neutral Ge transitions using the 304, 288, 265, and 252 nm emission lines, the minimum detectable atomic emission occurred near 0.5 J cm^{-2}.

B. Plume emission characteristics

Time-integrated emission spectra of a plume generated by irradiating a GeO_2 target with a laser fluence of 6.5 J cm^{-2} at a base pressure of 4×10^{-6} Torr are shown in Fig. 3. The transitions associated with each spectral feature in this figure are listed in Table I. This figure illustrates the dramatic change in the plasma emission as the collection position is changed from the target surface to 5 cm away. At $z=0.2$ cm, the emission consisted of features associated with both Ge I and Ge II atoms superimposed onto a continuum background. The ion lines appeared very broad and had intensities comparable to the neutral line intensities. The continuum background significantly decreased and the Ge I emission lines became much narrower 1 cm away from the target surface. The Ge II features were reduced in intensity relative to the neutral lines and remained broad. At 3 cm from the "0" position, the emission was dominated by Ge I transitions with a small contribution from the ionic species. Finally, the Ge II features disappeared at $z=5$ cm and the plume radiated solely from electronically excited states of Ge I atoms.

The discrete emission lines observed in this study primarily consisted of transitions originating from electronic states involving neutral and singly ionized Ge atoms. Most of the neutral transitions originated from the $4p^2$–$4p5s$ configuration. As shown in Table I, however, transitions originating from higher lying electronic states in Ge I were detected in

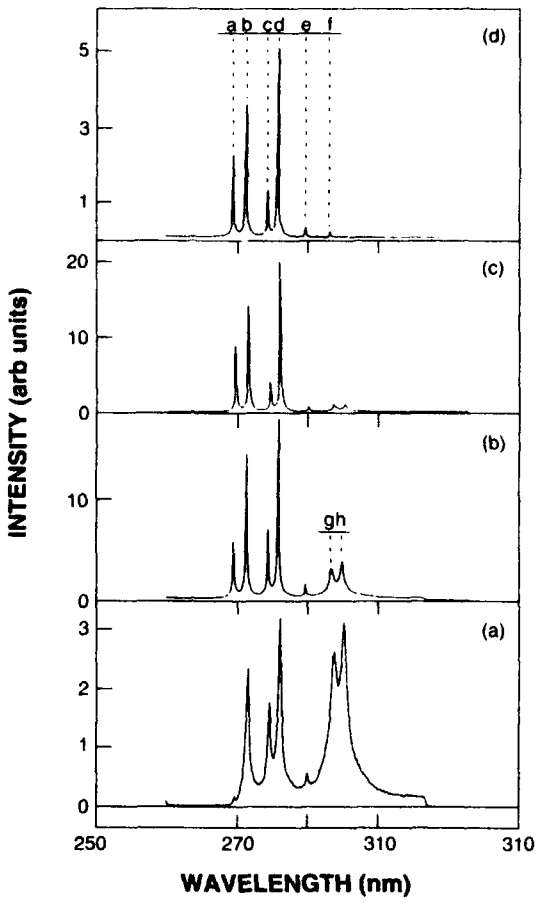

FIG. 3. Plasma emission spectra of material ablated from a GeO_2 target in vacuum (4×10^{-6} Torr) at $F=6.5$ J cm^{-2}. The spectra are labeled according to distance from the target surface: (a) $z=0.2$ cm, (b) $z=1.0$ cm, (c) $z=3.0$ cm, and (d) $z=5.0$ cm. The transitions labeled a–h are summarized in Table I. Although the intensities have arbitrary units, the relative magnitudes are preserved in the plots in order to compare line intensities at different locations.

these plumes. The emissions from Ge II were comprised of the following transitions: $5s^2S$–$5p^2P^0$, $5p^2P^0$–$6s^2S$, $5p^2P^0$–$5d^2D$, and $4d^2D$–$4f^2F^0$. Higher-energy transitions associated with Ge III could not be observed due to the detection limits imposed by the spectrometer and the diode array. Examination of the spectrum at long wavelengths also

TABLE I. Details of the atomic transitions[a] associated with the emission lines depicted in Fig. 3.

Label	Species	Transition wavelength (nm)	Transition	E_{lower} (cm^{-1})	E_{upper} (cm^{-1})
a	Ge I	269.13	$4p^2\ ^3P_1$–$5s^3P_1$	557	37 702
b	Ge I	270.96	$4p^2\ ^3P_1$–$5s^3P_0$	557	37 452
c	Ge I	274.04	$4p^2\ ^1S_0$–$4d^1P_1$	16 367	48 962
d	Ge I	275.46	$4p^2\ ^3P_2$–$5s^3P_1$	1410	37 702
e	Ge I	279.39	$4p^2\ ^1S_0$–$6s^3P_1$	16 367	52 148
f	Ge I	282.90	$4p^2\ ^1S_0$–$4d^1P_1$	16 367	51 705
g	Ge II	283.18	$4p^2\ ^2D_{3/2}$–$4f^2F_{5/2}$	65 015	100 317
h	Ge II	284.55	$4p^2\ ^2D_{5/2}$–$4f^2F_{7/2}$	65 184	100 316

[a]From Ref. 16.

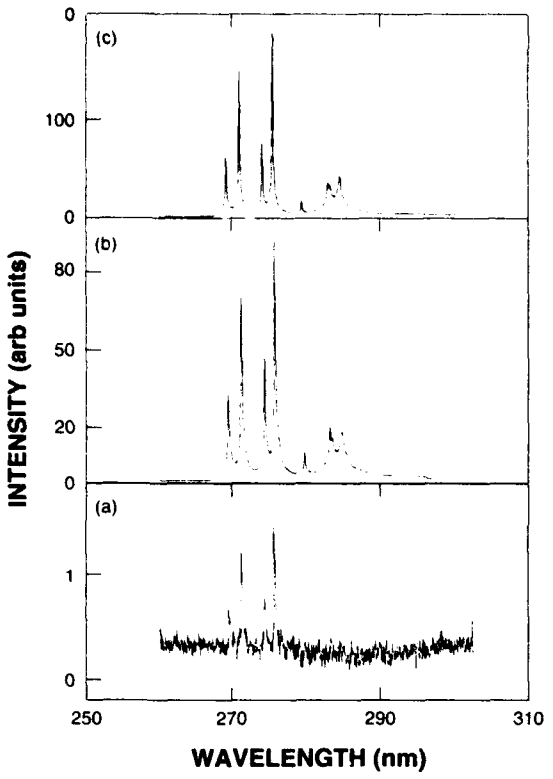

FIG. 4. Plume emission features recorded at three laser fluences: (a) 0.5 J cm^{-2}, (b) 1.0 J cm^{-2}, and (c) 6.5 J cm^{-2}. The spectra were obtained in vacuum at $z=1$ cm.

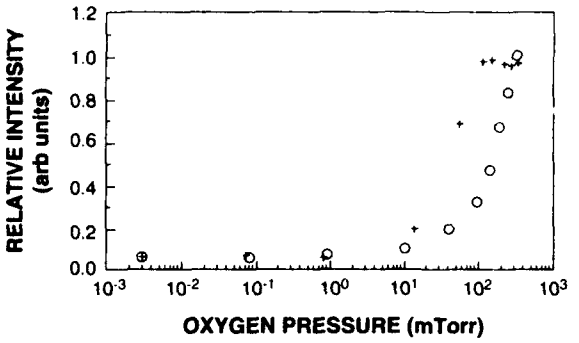

FIG. 5. Relative intensity behavior of the Ge I 269.1 nm emission line (+) and the Ge II 283.2 nm emission line (○) as a function of the oxygen pressure. The Ge I intensities are obtained at $z=3$ cm and the Ge II intensities are recorded at $z=1$ cm. Both data have been obtained with a laser fluence of 6.5 J cm^{-2}. These trends are common to all other neutral and ion Ge emissions recorded in these studies.

revealed emissions originating from electronically excited, neutral atomic oxygen (O*I). (Note: the * symbol will be used to specifically designate electronically excited states.) Molecular emission from GeO was not detected under any of the conditions utilized in these experiments.

The main spectral features of the plume remained the same over the range of fluences utilized in this work. That is, the nature of the emitting states from the neutral species and ions with the same degree of ionization did not change with distance from the target surface regardless of laser fluence. However, the intensities of the atomic lines were sensitive to the laser fluence as illustrated in Fig. 4. No discrete ion emission features were observed at $F<1$ J cm^{-2} regardless of the position from the target surface or the pressure of the ambient gas. However, neutral emission did appear at laser fluences as low as 0.5 J cm^{-2} but the emission was extremely weak at $z\leq 0.5$ cm. Since no ion state emission was observed at these laser fluences, the electronically excited neutrals were presumably dissociated directly from the target surface and these states were probably not formed via ion recombination reactions. Continuum emission, which has been frequently observed in laser generated plumes near the target surface, was conspicuously absent during ablation in vacuum at $F\leq 1$ J cm^{-2}. As the fluence increased from 0.5 to 1.0 J cm^{-2}, the neutral line intensities increased by a factor of 15 while a much slower increase (factor of 2) was observed between 1.0 and 6.5 J cm^{-2} for both the Ge I and Ge II emission lines. Although the intensities of the individual atomic lines varied with laser fluence, the relative intensities of spectral features remain unchanged. This implied that the local equilibrium was maintained among the energy levels regardless of the laser fluence.

The presence of an ambient gas dramatically affected the plasma characteristics. Figure 5 summarizes the general trend in the relative emission intensities versus O_2 pressure. The neutral line intensities in this figure were recorded at $z=3$ cm while the ion data were obtained at $z=1$ cm and both data sets were produced with a laser fluence of 6.5 J cm^{-2}. The intensities of both Ge I and Ge II lines, which were proportional to the excited state number densities of the respective species, remained relatively constant over four orders of magnitude change in O_2 pressure. The neutral emission intensities increased by a factor of 10 between 10 and 100 mTorr, and subsequently approached a constant value above 100 mTorr of added O_2. Clearly, the higher oxygen pressures caused a considerable enhancement in the neutral populations. The ion emission behavior was different at O_2 pressures above 10 mTorr: the ion state intensity monotonically increased but showed no indication of leveling or decreasing at the highest pressures used in these studies. The intensities recorded at 120 mTorr were a factor of 10 greater than those obtained at the lowest pressures. Similar trends were observed for data recorded with a laser fluence of 1 J cm^{-2} for both Ge I and Ge II.

The dynamics of laser produced plumes are partially governed by the backing pressure of an ambient gas.[20] In vacuum,[21] the plume is allowed to expand freely in a forward-directed pattern with a $(\cos\theta)^n$ functional dependence, where n typically ranges from 10 to 40. However, the propagation of the plume is modified even at moderate backing pressures resulting in a narrowing of the plume and a subsequent increase in n to a value as high as 200. In this study, the addition of 100–150 mTorr of O_2 forced the plume to appear constricted and more spatially confined than in vacuum. This effect could cause the number of emitters per unit volume to increase within the observation region resulting in an apparent increase in the emission intensities at higher O_2 pressures. This mechanism, which could account

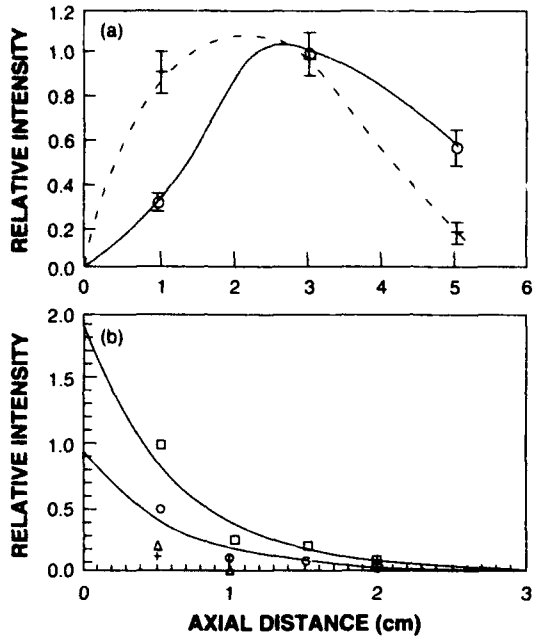

FIG. 6. The relative line intensities of Ge I and Ge II vs distance from the target surface: (a) shows the Ge I (312.5 nm transition) behavior at two pressures (+) vacuum and (○) 200 mTorr of O_2; (b) illustrates the Ge II (602.1 nm transition) dependence in vacuum (+), $P(O_2)=1$ mTorr (△), $P(O_2)=84$ mTorr (○), and $P(O_2)=170$ mTorr (□). A laser fluence of 6.5 J cm^{-2} has been utilized to obtain these data. All other neutral and ion emission features follow the trends depicted in this figure.

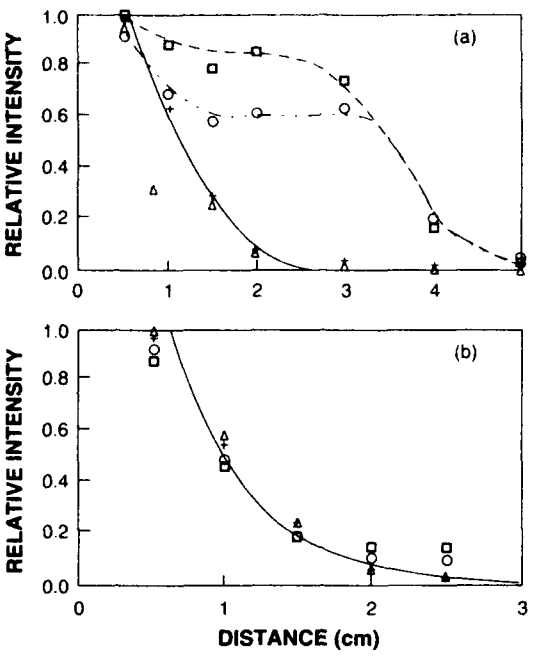

FIG. 7. The evolution of the 844.6 nm atomic oxygen line vs distance from the target surface at $F=6.5$ J cm^{-2}: (a) illustrates the behavior in O_2 while (b) shows the effect of N_2 as the ambient gas. The gas pressures in each figure are: (+) vacuum, (△) 1 mTorr, (○) 84 mTorr, and (□) 170 mTorr. All data have been normalized to the intensity measured at $z=0.2$ cm.

for the trends displayed in Fig. 5, was tested by simulating a change in the pressure gradient in the plume by using different laser spot sizes at a constant fluence. A tight laser focus causes a high-pressure gradient across the plume which forces a stronger expansion than a softer focus at the same fluence. Thus, focusing the laser spot more softly should produce a similar effect as that created by increasing the background gas; namely, the shorter extent of the expansion should keep more emitting atoms confined to a smaller volume. Under these conditions, the experiments showed that the ratios of spectral line intensities for the soft focus to the tight focus increased by 10%–30%. Spatial confinement could partially account for the pressure-dependent intensities, but other processes uncovered after examining the behavior of the oxygen atom line intensities versus O_2 pressure may dominate as discussed below.

Figure 6 shows relative axial intensity distributions at successive distances from the target surface at two pressures. In Fig. 6(a), the Ge I line intensities recorded in vacuum reached their maximum values 1.5–2.0 cm from the target surface and the position of the maximum intensity shifted to 2.5–3.0 cm at an O_2 pressure of 200 mTorr. Although the data were recorded only at $z\leq 5$ cm, the emission was observable to at least 7 cm from the target surface at all pressures. The ion emission, however, had a peak intensity near the target surface and exponentially decayed over distance as illustrated in Fig. 6(b). In vacuum, the ion emission was recorded out to ~0.5–1.0 cm from the target surface, where the signal levels fell below the detection limits of the experiment, whereas increases in the O_2 pressure resulted in detectable signals as far out as $z=3$ cm. Exponential density profiles have been used in gas dynamic simulations in the adiabatic expansion region of a plasma,[22] and these results may support this picture of a nonthermal plume expansion. The laser fluences affect the intensity distribution only to a minor extent; the brightest regions of the plume appear in the same location and to the same extent.

The trends observed for atomic oxygen are contrary to those observed with Ge. Figure 7(a) shows the evolution of the 844.6 nm emission line from atomic oxygen. In the O_2 pressure range 0 mTorr$\leq P(O_2)\leq$1 mTorr, the O I emission rapidly decreased to negligible values at ~3 cm from the target surface. The O I emission observed under these conditions was clearly a product of electronic excitation of atomic oxygen due to the ablation process because, at these pressures, the relatively low collision frequency prohibited any significant interaction between the oxygen added to the chamber and the plume material. At higher pressures, however, the O I emission intensity displayed a small decrease but attained a constant value in the region 1.5 cm$\leq z\leq$3 cm. The O*I populations subsequently decayed at $z>3$ cm and finally became undetectable near $z=5$ cm. The behavior of the emissions at higher pressures could be caused by an increased residence time in the observation region as discussed previously. However, the 40 ns radiative lifetime of this transition ($^3S_0-^3P$) limited the travel distance to ≤1 mm before decaying, assuming a typical velocity of 10^6 cm s^{-1} found in laser generated plumes. The high-pressure results demonstrated that additional O*I production mechanisms must exist to account for the observed behavior.

In order to better understand the intensity behavior described in Fig. 7(a), the O I emission was monitored as a function of N_2 pressure to check whether or not additional excited oxygen atoms were being produced in reactions between the plume material and the ambient molecular oxygen. Figure 7(b) shows that the relative O*I number density remained constant at a fixed location from the target as the N_2 pressure increased from 0 to 150 mTorr. However, the O I emission decreased exponentially with distance with the same functional dependence at each pressure. Thus, the presence of O_2 acted as a source of additional atomic oxygen and this trend also revealed that the O*I dependence on the O_2 pressure was not a residence time effect.

IV. DISCUSSION

The ablation of GeO_2 glass can be partially explained by considering the optical and thermal properties of the irradiated material. The removal of material from a target by laser irradiation depends on the coupling efficiency of the laser beam energy to the target. The absorption coefficient, α of GeO_2 at 6.4 eV (193 nm) is 2×10^5 cm^{-1} which corresponds to an absorption depth of ~50 nm.[19] For "congruent evaporation," the heat diffusion distance δ must be smaller than the absorption depth. We can estimate the heat diffusion depth using typical values for the thermal conductivity[23,24] ($K=0.015$ W cm^{-1} K^{-1}) and the specific heat[25] ($C_p=0.19$ cal g^{-1} K^{-1}) for glass at 300 K. On a time scale comparable to the laser pulse duration ($\tau=28$ ns), $\delta[=(2D\tau)^{1/2}]$ is calculated to be ~170 nm, where $D=K/\rho C_p$ and $\rho=3.68$ g cm^{-3} for GeO_2 glass.[25] Thus, the energy absorbed during the laser irradiation time is confined to a surface layer corresponding to the thermal diffusion length.

When energy densities above the vaporization threshold are applied to the target, the laser energy is not only absorbed in a surface layer of ≈50 nm but intense local heating also occurs within a distance of 170 nm which can lead to additional material vaporization. In these experiments, the laser ablation threshold was near 0.46 J cm^{-2} based on the results of both the optical emission studies and crater formation on the target surface. The surface temperature on the target is estimated at this fluence using a simplified approximation to the heat diffusion equation in one dimension described by Ready[26] given in Eq. (2).

$$T(z=0,\tau)=(2\Phi_0/K)(D\tau/\pi)^{1/2}, \tag{2}$$

where $\Phi_0=(\Phi/\tau)(1-R)$, Φ is the laser flux, and R is the reflectivity ($R\approx0.12$–0.13 for GeO_2 at 6.4 eV).[19] Using the thermodynamic values defined above, the upper limit to the surface temperature at the end of the laser pulse for a fluence of 0.46 J cm^{-2} is ~7000 K. This value is greater than the liquid transition temperature ($T_{liq}\approx2625$ K) for GeO_2, so removal of material from the target should occur within the thermal diffusion length. By scaling $T(z=0,\tau)$ with Φ, Eq. (2) suggests that ablation threshold may be lower than 0.46 J cm^{-2}. In order to achieve the liquid transition temperature of GeO_2, Eq. (2) predicts that the laser must deposit an energy density of 200 mJ cm^{-2}.

The interaction of the laser with the solid surface produces electrons and ions in addition to copious amounts of neutrals. The number density of these species has a complex evolution and they depend on the irradiation conditions, the collisional kinetics in the plume, and the distance from the target surface. The most important result of this study is the pronounced effect on the plume's luminescence and, thus, the number densities of individual species, caused by the presence of molecular oxygen. At O_2 pressures below 10 mTorr, both Ge*II and O*I decay exponentially from the target surface. In addition, the Ge I emission peaks when the Ge*II and O*I concentrations reach their minimum values near $z=2$ cm. These results imply the existence of a neutral-ion conversion mechanism to explain the delayed peaking of the Ge I emission intensity. At these low pressures, the equilibrium mean-free path (MFP) between O_2 and Ge is >1 cm so collisional interactions between these species or other plume constituents with the ambient could be eliminated. Therefore, electron-ion or electron-atom interactions within the plume may explain the increase in the Ge*I number density at the expense of the ions and atomic oxygen.

Both the neutral and ion state concentrations begin to increase near 20–30 mTorr of added O_2. This threshold also coincides with an increase in the O I emission. At these pressures, the MFP is typically 1–2 mm; thus, the increase in the neutral atom concentrations appear to be linked with higher collision frequencies which makes the reaction Ge(I or II)+O*I→Ge*(I or II)+O more probable. The ion emission, however, remains confined to within about 1–1.5 cm of the target surface where electron densities are higher which possibly promote e^--atom ionization processes to account for the increase in the ion state populations.

The ablation of GeO_2 at high ambient pressures [$P(O_2)>10$ mTorr] not only produces O*I directly as a result of the ablation process, but also increases the excited O atom concentration through plume-O_2 interactions. The magnitude of the cross sections for e^--O_2 collisions resulting in the dissociation of O_2 into various excited atomic products range from 2.2×10^{-17} to 6.6×10^{-17} cm^2 for electron energies ranging between 13.5 and 33.5 eV.[27] These values translate into relatively efficient collisional dissociation if the electron kinetic energies are in the appropriate range. The ablation of targets containing Ge is known to produce atomic species with average kinetic energies of 40–100 eV.[15,28] The accompanying electrons are expected to have higher kinetic energies than the atomic species which makes O_2 dissociation by electron impact highly probable.

The maximum emission intensity is determined by the collisional excitation mechanisms and the radiative lifetimes at the higher ambient gas pressures. Collisional interactions between the plume and the ambient O_2 clearly increase the concentrations of excited Ge I and Ge II over those observed at the low ambient pressures. In addition to e^--atom collisions which can produce more ions in the plume, excited O atoms can interact with Ge atoms to produce electronically excited Ge. The presence of an O*I creation process, therefore, makes this event more probable. The excited species are also observed farther from the target surface at high pressures which implies that the processes responsible for production of these excited states have a spatial dependence.

The results of this study impact the understanding of

stoichiometric GeO_2 thin-film formation. Different deposition conditions typically lead to variations in plasma luminescence and the details of the emission spectra can identify conditions for producing high-quality thin films. In an earlier work,[14] we found that stoichiometric GeO_2 thin films could be produced at high ambient O_2 pressures (150 mTorr). Furthermore, these studies showed that stoichiometric films were produced only when the substrate was physically located within the plume and films grown outside the plume have been found to be oxygen deficient. The results presented here demonstrate that high pressures of O_2 increase the number density of excited neutrals atoms and excited ion states. This implies that the higher-energy content of the plume is necessary for producing quality films. By placing the substrate within the plume [typically 4 cm at $P(O_2)=150$ mTorr], the substrate is bombarded by O I, Ge I, and Ge II atoms in various electronic states as well as by molecular oxygen in the ambient. Reactions of these species in the gas phase and/or on the substrate surface promote the proper oxygen incorporation in these films.

V. CONCLUSIONS

The plume generated from 193 nm irradiation of GeO_2 targets was examined by recording dispersed emission in the UV to visible regions. The emission spectra were recorded as a function of laser fluence, distance from the front surface of the target, and molecular oxygen pressure. The ablation rate of GeO_2 was also determined in this work. Neutral and singly ionized atomic species were observed in the plume and the emission intensities of these species depended on both the O_2 pressure and distance from the front surface of the target. The behavior of the emission intensities of these species were directly connected to the excited atomic oxygen concentrations which was produced as a by-product of the ablation process in vacuum and as a product of plume-O_2 interactions at higher ambient gas pressures. The change in the plume's concentration of excited species by ambient O_2 affected the film growth by producing additional energetic species that impacted the substrate which subsequently incorporated stoichiometric proportions of oxygen in the film structure. Because the excited species responsible for the plume luminescence represents only a small fraction of the material removed from the target, we are currently utilizing laser induced fluorescence to obtain information on the dynamics and kinetics of the nonemitting species in the plasma.

ACKNOWLEDGMENTS

I would like to thank Steven Ramsey for his technical assistance during these experiments and the fruitful discussions with Dr. Brian Patterson and Dr. Sarath Witanachchi.

[1] J. T. Cheung and H. Sankur, CRC Crit. Rev. Solid State Mater. Sci. **15**, 63 (1988).
[2] G. Mehlman, D. B. Chrisey, P. D. Burkhalter, J. S. Horwitz, and D. A. Newman, J. Appl. Phys. **74**, 53 (1993).
[3] G. Mehlman, D. B. Chrisey, J. S. Horwitz, P. D. Burkhalter, R. C. Y. Auyeung, and D. A. Newman, Appl. Phys. Lett. **63**, 2490 (1993).
[4] Q. Y. Ying, D. T. Shaw, and H. S. Kwok, Appl. Phys. Lett. **53**, 1762 (1988).
[5] X. D. Wu, B. Dutta, M. S. Hegde, A. Inam, T. Venkatesan, E. W. Chase, C. C. Chang, and R. Howard, Appl. Phys. Lett. **54**, 179 (1989).
[6] O. Auciello, S. Athavale, O. E. Hankins, M. Sito, A. F. Schreiner, and N. Biunno, Appl. Phys. Lett. **53**, 72 (1988).
[7] G. Koren, A. Gupta, and R. Bassman, Appl. Phys. Lett. **54**, 2035 (1989).
[8] P. E. Dyer, A. Issa, and P. H. Key, Appl. Phys. Lett. **57**, 186 (1990).
[9] J. Seth, R. Padiyath, and S. V. Babu, Appl. Phys. Lett. **63**, 126 (1993).
[10] H. Sankur, J. G. Nelson, A. J. Pritt, Jr., and W. J. Gunning, J. Vac. Sci. Technol. A **5**, 15 (1987).
[11] P. J. Wolf, J. Appl. Phys. **72**, 1280 (1992).
[12] J. T. Knudtson, W. B. Green, and D. G. Sutton, J. Appl. Phys. **61**, 4771 (1987).
[13] S. Deshmukh, E. W. Rothe, and G. P. Reck, J. Appl. Phys. **66**, 1370 (1989).
[14] P. J. Wolf, T. M. Christensen, N. G. Coit, and R. W. Swinford, J. Vac. Sci. Technol. A **11**, 2725 (1993).
[15] F. Vega, C. N. Afonso, and J. Solis, J. Appl. Phys. **73**, 2472 (1993).
[16] J. Reader, C. H. Corliss, W. L. Wiese, and G. A. Martin, "Wavelength and Transition Probabilities for Atoms and Atomic Ions," NSRDS-NBS 68 Parts I, II, Washington, DC, 1980; M. M. Miller and R. A. Roig, Phys. Rev. A **7**, 1208 (1973); J. Lotrain, J. Cariou, Y. Guern, and A. Johannin-Gilles, J. Phys. B **11**, 2273 (1978).
[17] G. A. Capelle and J. M. Brom, Jr., J. Chem. Phys. **63**, 5168 (1975).
[18] W. L. Wiese, M. W. Smith, and B. M. Glennon, "Atomic Transition Probabilities," NSRDS-NBS-4, Vol. I, Washington, DC, 1966.
[19] L. Pasajova, Czech. J. Phys. B **19**, 1265 (1969).
[20] D. B. Geohegan, Appl. Phys. Lett. **60**, 2732 (1992).
[21] D. J. Lichtenwalner, O. Auciello, R. Dat, and A. I. Kingon, J. Appl. Phys. **74**, 7497 (1993).
[22] R. K. Singh and J. Narayan, Phys. Rev. B **41**, 8843 (1990).
[23] *Handbook of Physics* (McGraw–Hill, New York, 1958).
[24] *Handbook of Chemistry and Physics*, 65th ed. (CRC, Boca Raton, FL, 1984).
[25] N. M. Ravindra, R. A. Weeks, and D. L. Kinser, Phys. Rev. B **36**, 6132 (1987).
[26] J. F. Ready, *Effects of High-Power Laser Radiation* (Academic, New York, 1971), p. 73.
[27] P. C. Cosby, J. Chem. Phys. **98**, 9560 (1993).
[28] D. Lubben, S. A. Barnett, K. Suzuki, S. Gorbatkin, and J. E. Greene, J. Vac. Sci. Technol B **3**, 968 (1985).